Determinant quantum Monte Carlo study of exhaustion in the periodic Anderson model

Lufeng Zhang,[1] Tianxing Ma,[1,*] Natanael C. Costa,[2,3] Raimundo R. dos Santos,[3] and Richard T. Scalettar[4]
[1]*Department of Physics, Beijing Normal University, Beijing 100875, China*
[2]*International School for Advanced Studies (SISSA), Via Bonomea 265, 34136 Trieste, Italy*
[3]*Instituto de Física, Universidade Federal do Rio de Janeiro, Caixa Postal 68528, 21941-972 Rio de Janeiro, RJ, Brazil*
[4]*Physics Department, University of California, Davis, California 95616, USA*

(Received 27 March 2019; revised manuscript received 14 May 2019; published 28 May 2019)

The Kondo and periodic Anderson models describe many of the qualitative features of local moments coupled to a conduction band, and thereby the physics of materials such as the heavy fermions. In particular, when the exchange coupling J or hybridization V between the moments and the electrons of the metallic band is large, singlets form, quenching the magnetism. In the opposite, small J or V, limit, the moments survive and the conduction electrons mediate an effective interaction which can trigger long-range, often antiferromagnetic order. In the case of the Kondo model, where the moments are described by local spins, Nozières considered the possibility that the available conduction electrons within the Kondo temperature of the Fermi surface would be insufficient in number to accomplish the screening. Much effort in the literature has been devoted to the study of the temperature scales in the resulting "exhaustion" problem and how the "coherence temperature" where a heavy Fermi liquid forms is related to the Kondo temperature. In this paper, we study a version of the periodic Anderson model in which some of the conduction electrons are removed in a way which avoids the fermion sign problem and hence allows low-temperature quantum Monte Carlo simulations which can access both singlet formation and magnetic ordering temperature scales. We are then able to focus on a somewhat different aspect of exhaustion physics than previously considered: the effect of dilution on the critical V for the singlet-antiferromagnetic transition.

DOI: 10.1103/PhysRevB.99.195147

I. INTRODUCTION

A fundamental property of the description of a local magnetic moment embedded in a sea of conduction electrons provided by the Kondo model (KM) and the single impurity Anderson model (SIAM) [1] is the screening of the moment through the formation of a Kondo singlet, a phenomenon which occurs below a characteristic Kondo temperature T_K. This singlet formation is accompanied by the appearance of a narrow resonant state at the Fermi energy and a large electronic effective mass, enabling these models to provide a qualitative picture of heavy fermion physics—the enhancement of specific heat and magnetic susceptibility [2–4]. Certain features of this problem are amenable to exact analytic solution, e.g., via the Bethe ansatz [5,6].

The periodic Anderson model (PAM) extends the single impurity problem to the dense limit, i.e., to a lattice of magnetic moments, raising the possibility of the emergence of magnetic ordered states. This may occur due to an indirect coupling between local moments mediated by the conduction-electron polarization (oscillations of the spin density), which is known as the Ruderman-Kittel-Kasuya-Yosida (RKKY) interaction [7–9]. The Fermi wave vector k_F of the conduction electrons determines the oscillation wavelength between moments separated by distance R, $J_{RKKY}(R) \sim [k_F \cos(2k_F R)]/R^3$. Thus the density of conduction electrons n_c, via k_F, plays a crucial role in the magnetic ordering pattern [10–14]. Due to its importance to heavy fermion physics, the competition between singlet formation and the magnetic ordering has been investigated through many different methods, from analytical [15–19] to numerical [20–32]. In particular, quantum Monte Carlo (QMC) simulations [20,31] have provided evidence of the existence of a quantum phase transition from a staggered antiferromagnetic phase to a spin-liquid state in the two-dimensional PAM at half filling.

This competition is strongly affected by the electronic density: as n_c is reduced, fewer conduction electrons are available to screen the local moments. Indeed, Nozières introduced the idea of "exhaustion" to describe the increased difficulty in singlet formation. Even when, naively, n_c is large, only conduction electrons within $k_B T$ of the Fermi surface are available for screening. Thus, Nozières suggested that the singlet formation would occur at an energy scale called the "coherence temperature" T_{coh}, much lower than the Kondo temperature of the SIAM. In this picture, a particular functional form $T_{coh} \sim N(E_F)\, T_K^2/N_{imp}$, where $N(E_F)$ is the density of states at the Fermi energy and N_{imp} is the number of local moments, reflects the availability of only those conduction electrons within T_K of the Fermi surface.

Considerable numerical effort [16,25,33,34] has gone into evaluating T_{coh} and its relation to T_K, specifically on the validity of Nozières' original suggestion $T_{coh} \sim T_K^2$. The situation is potentially complex for a number of reasons. First, the singlets formed at this scale could be rather different from those envisioned in the simpler SIAM where a single f

*Corresponding author: txma@bnu.edu.cn

 ©2019 American Physical Society

moment is screened by conduction electrons. Instead, below $T_{\rm coh}$, a much more complex tangle of spin correlations might emerge in which f electrons also screen each other, i.e., singlets between f electrons develop. Second, for the PAM, there are additional energy scales associated with f electron charge fluctuations. In this case, it has been found [25] that the detailed relation $T_{\rm coh} \sim N(E_{\rm F})T_{\rm K}^2/[\alpha(U_f, V)N_{\rm imp}]$ is also affected by the scales of the on-site U_f and interband hopping V energies, as opposed to a simple counting of the relative numbers of conduction and local electrons. Despite the great experimental and theoretical effort [35–44], the exact relation between these two energy scales ($T_{\rm K}$ and $T_{\rm coh}$) is still an open question.

Finally, it has been suggested [33,45] that the physics of exhaustion might be fundamentally different depending on the strength of the coupling between the conduction electrons and local moments. For large couplings, the singlets are local and dilution of conduction electrons leaves behind well-defined local "bachelor spins," which must then find a way to form singlets. For small couplings, the screening is largely collective in the first place, even before conduction-electron dilution. This would suggest that the nature of exhaustion differs markedly at small and large V, in line with a more complex relation between $T_{\rm coh}$ and $T_{\rm K}$ described in Ref. [25].

In this work, our main interest is to investigate how the dilution of conduction electrons affects the response of magnetic quantities in the PAM. In particular, and differently from previous work [46–48], we are interested in determining the evolution of the quantum critical point (QCP) when the number of conduction electrons differs from the localized ones, that is, $n_c \neq n_f$. In addition, we do not rely on Pauli blocking, i.e., the restriction of conduction-electron excitations to a temperature window around $E_{\rm F}$. Instead, we directly remove orbitals and their associated electrons in order to introduce depletion. In so doing, we can examine not just Nozière's original exhaustion limit, when the ratio $p = n_c/n_f < 1$, but the opposite case, $p = n_c/n_f > 1$, as well. This problem is investigated with the aid of an exact numerical approach, namely, the determinant quantum Monte Carlo (DQMC) method [49–54], by introducing a model which allows us to control the ratio $p \equiv n_c/n_f$ without running into the sign problem [55,56]. The description of the model and the methodology are presented in the next section. Our results are shown in Sec. III, while our main conclusions are summarized in Sec. IV.

II. MODEL AND NUMERICAL METHOD

Our work is focused on the PAM, whose Hamiltonian in real space reads

$$\hat{H} = -\sum_{\langle i,j\rangle\sigma} t_{ij}(c^\dagger_{i\sigma}c_{j\sigma} + \text{H.c.}) - \sum_{\langle i,j\rangle\sigma} V_{ij}(c^\dagger_{i\sigma}f_{j\sigma} + \text{H.c.}) + U_f\sum_{\mathbf{i}}\left(n^f_{i\uparrow} - \frac{1}{2}\right)\left(n^f_{i\downarrow} - \frac{1}{2}\right) - \mu\sum_{\mathbf{i}} n_{\mathbf{i}}. \quad (1)$$

Here, $c^\dagger_{i\sigma}$ ($c_{i\sigma}$) and $f^\dagger_{i\sigma}$ ($f_{i\sigma}$) are the creation (annihilation) operators of conduction and localized electrons, respectively, in the standard second quantization formalism. Similarly, $n^c_{\mathbf{i}\sigma}$ and $n^f_{\mathbf{i}\sigma}$ are site-number operators for c and f electrons, with $n_{\mathbf{i}} = \sum_\sigma (n^f_{\mathbf{i}\sigma} + n^c_{\mathbf{i}\sigma})$ being the total occupation on site $\mathbf{i}$. t_{ij} denotes the nearest-neighbor (NN) hopping between c electrons, and V_{ij} represents the nonlocal hybridization between f orbitals and its NN conduction sites. In the f-orbital dilution case, when the f electron is removed from site $\mathbf{i}$, $V^{f\to c}_{ij} = 0$ ($j \in \langle i, j\rangle$), as Fig. 1(b) shows. On the other hand, if the c electron on site $\mathbf{i}$ gets diluted, we set $t_{ij} = 0, V^{c\to f}_{ij} = 0$ ($j \in \langle i, j\rangle$) as the exhaustion case plotted in Fig. 1(c). Figure 1(a) illustrates the nonlocal nature of the hybridization for the undiluted geometry; here, for simplicity, just the one-dimensional analog is shown. The local character of f sites is denoted by the momentum independence of the f level, ϵ_f, and by the strong Coulomb repulsion U_f for doubly occupied orbitals. We set $t = 1$ as the energy scale and explore the "symmetric limit," $\mu = \epsilon_f = 0$, for which the density of the c and f electrons is half filled, $\langle n^c_{i\sigma}\rangle = \langle n^f_{i\sigma}\rangle = \frac{1}{2}$, a property which holds for all t, U_f, V, and temperatures T, due to the particle-hole symmetry (PHS) of a bipartite lattice with NN hopping terms.

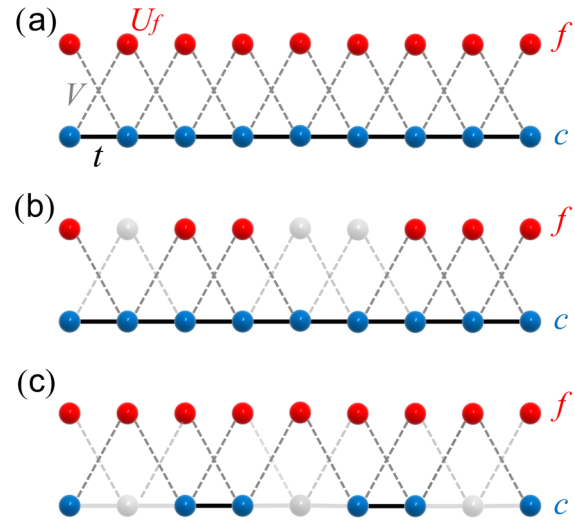

FIG. 1. One-dimensional representation of the geometry of our Hamiltonian. (a) The undiluted case in which all conduction (c) and local (f) orbitals are present. Bold horizontal lines are associated with the conduction hopping t, and dashed diagonal lines with the conduction-local-electron hybridization V. Both connect near-neighbor sites. (b) Several of the f orbitals, and their associated hybridizations V to the conduction orbitals, removed. (c) Analogously, several of the conduction orbitals removed. This is the case most relevant to a study of exhaustion.

At this point, we should mention that on-site (local) hybridizations are more commonly studied rather than those with NN couplings, such as the doping effect of the on-site hybridization PAM [57]. Then, it is worth emphasizing the differences between both cases beyond their dispersive character. While the former leads to a charge gap for the noninteracting limit ($U_f = 0$) at half filling, the latter is a metal for any hybridization strength. As a consequence, the dispersive $V_{\mathbf{k}}$ is more appropriate to describe a metallic system [58,59]. Further, in the case of on-site hybridization and $U_f \neq 0$, there is evidence of conduction-electron localization when

f orbitals are removed, accompanied by an enhancement of spin-spin correlations around the unpaired noninteracting sites, breaking singlets and leading to a magnetic ground state even at large V [60–64]. This effect may overestimate the magnetic response, in particular, the value of the critical hybridization for a given interaction strength, $V_c(U_f)$. By contrast, such effects are strongly attenuated in the dispersive case since unpaired sites are less likely in a more connected lattice, as in the case of nonlocal hybridization. In view of this, the latter seems more relevant to study the evolution of the critical point in diluted systems.

The properties of the model are investigated using the determinant quantum Monte Carlo method [49–51], which allows for an exact solution (to within statistical sampling errors) of the PAM Hamiltonian on finite-size lattices. Here we present highlights of the method, the details of which can be found in a number of reviews; see, e.g., Refs. [52–54]. The underlying step is the construction of a path integral for the partition function $\mathcal{Z}$ by discretizing the inverse temperature $\beta = L\Delta\tau$, and breaking the full imaginary-time evolution operator $e^{-\beta\hat{H}}$ into incremental pieces $e^{-\Delta\tau\hat{H}}$. This allows for the use of the Trotter approximation [65–67], $e^{-\Delta\tau\hat{H}} \sim e^{-\Delta\tau\hat{K}}e^{-\Delta\tau\hat{\mathcal{U}}}$, which isolates the interaction term $\hat{\mathcal{U}}$, containing U_f, from the quadratic kinetic-energy pieces containing t, μ, and V.

The interacting $\hat{\mathcal{U}}$ term is decoupled in a quadratic form by performing a discrete Hubbard-Stratonovich (HS) transformation, with the inclusion of auxiliary fields $S(\mathbf{i},\tau)$ in both real and imaginary coordinates, that are coupled to the spin of electrons. Therefore, the path integral consists entirely of quadratic forms and the fermionic trace can be evaluated, resulting in a trace over HS fields of a product of determinants, $\det\mathcal{M}_\uparrow(\{S(\mathbf{i},\tau\}) \det\mathcal{M}_\downarrow(\{S(\mathbf{i},\tau)\})$, of matrices whose dimension is the number of spatial sites of the lattice. The trace over $S(\mathbf{i},\tau)$ is carried out by sampling them through conventional Monte Carlo methods. Here, in addition to the usual single moves, we also perform global moves [68], which improves the ergodicity of the system.

Although the DQMC model is exact, it suffers from the infamous minus-sign problem [55,56], which arises from the possibility of the product $\det\mathcal{M}_\uparrow(\{S(\mathbf{i},\tau)\}\det\mathcal{M}_\downarrow(\{S(\mathbf{i},\tau)\}$ being negative for certain field configurations, corresponding to a negative density matrix. The sign problem is worse at low temperatures, large lattice sizes, or strong interactions, and its dependence with the electron filling or geometries is quite nontrivial [69,70]. However, this problem is absent for systems with PHS since it implies constraints over the two determinants, leading to a positive total sign. Notice that our Hamiltonian of Eq. (1) is particle-hole symmetric at half filling, and hence the sign problem is absent throughout this work.

As mentioned earlier, the system is diluted through the direct removal of orbitals and their associated electrons. In fact, the more obvious way to reduce conducting electrons would be by simultaneously setting $\mu < 0$ and $\epsilon^f < 0$ since it preserves the number of f electrons, but lowers the c occupancy. However, this leads to a severe sign problem and the energy scales for singlet formation and antiferromagnetic (AF) order are no longer accessible. By contrast, our approach preserves PHS, which only requires that the hopping and hybridization should be between NN sites at half filling, hence avoiding any sign problem. Figures 1(b) and 1(c) illustrate our dilution procedure for localized ($p = n_c/n_f > 1$) and conduction ($p = n_c/n_f < 1$) orbitals, respectively. We should also note that depletion affects the respective neighborhoods in different ways. With the concentration of c sites being $p = n_c/n_f < 1$, the probability that an f site is connected to $0 \leqslant m \leqslant 4$ active c sites is

$$P_m = \frac{4!}{m!(4-m)!}\, p^m(1-p)^{4-m}; \tag{2}$$

see the discussion of Figs. 8 and 9. In our measurements, for example, of the structure factor below, spatial configurations with isolated f electrons ($m = 0$) are not included since these sites contribute a "trivial" Curie-law free moment $\chi \sim 1/T$. Similarly, with the concentration of f sites being $q = n_f/n_c < 1$, the probability that a c site is connected to $0 \leqslant m \leqslant 4$ active f sites is also given by Eq. (2), but with p being replaced by q.

We investigate the magnetic properties by performing measurements of spin-spin correlation functions for f orbitals, and their Fourier transform, the spin structure factor,

$$\mathcal{S}^{\rm ff}(\pi,\pi) \equiv \frac{1}{N_{\rm f}}\sum_{\mathbf{i},\mathbf{j}} \langle\, S^{\rm f}_{\mathbf{i}} \cdot S^{\rm f}_{\mathbf{j}}\,\rangle (-1)^{\mathbf{i}+\mathbf{j}}, \tag{3}$$

where $N_{\rm f}$ is the number of f sites connected to at least one c site. Here, we define the fermionic spin operators as $\vec{S}^{\rm f}_{\mathbf{i}} = (f^\dagger_{\mathbf{i}\uparrow}, f^\dagger_{\mathbf{i}\downarrow})\,\vec{\sigma}\,(f_{\mathbf{i}\uparrow}, f_{\mathbf{i}\downarrow})^T$, with $\vec{\sigma}$ being the Pauli spin matrices; a similar expression applies to $\vec{S}^{c}_{\mathbf{i}}$. The phase factor $(-1)^{\mathbf{i}+\mathbf{j}}$ takes opposite signs on the two sublattices, corresponding to a staggered pattern.

For singlet formation, we examine a correlator function,

$$C^{fc}_{\mathbf{i}} \equiv \vec{S}^{\rm f}_{\mathbf{i}} \cdot {\sum_{\mathbf{j}\in\mathcal{N}(\mathbf{i})}}' \vec{S}^{\rm c}_{\mathbf{j}}, \tag{4}$$

with the sum being over sites $\mathbf{j}$ in the neighborhood $\mathcal{N}(\mathbf{i})$ of $\mathbf{i}$. The prime on the sum emphasizes that in the c-diluted case, some f orbitals have less than four c neighbors; see Eq. (2). By contrast, in the case of f dilution, every surviving f site necessarily has four neighboring c orbitals. The data reported here are obtained from lattice sizes up to $L = 12$, with averaging over 20 different disorder realizations. In general the requisite number of realizations in simulations with disorder must be determined empirically and is a complex interplay between self-averaging on sufficiently large lattices, the strength of the disorder, and the location in the phase diagram. We show the results in Fig. 2. For any dilution case, the averaged $S(\pi,\pi)$ are consistent regardless of the number of realizations. These plots justify the use of 20 realizations in our work. The error bars shown in the following results reflect both statistical and disorder sampling fluctuations.

III. RESULTS AND DISCUSSION

Let us first discuss the undiluted PAM [Fig. 1(a)], with which the diluted case should be compared. One should notice that due to the Mermin-Wagner theorem [71], long-range order is expected to occur only at $T = 0$. Therefore, as the

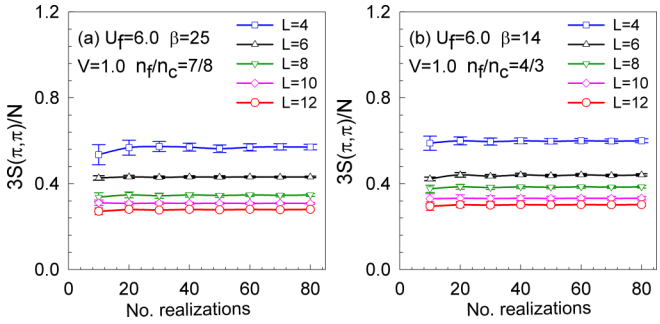

FIG. 2. AF spin structure factor $S(\pi,\pi)$ computed on the $L = 4, 6, 8, 10, 12$ lattices. At (a) $n_f/n_c = 7/8$ and (b) $n_f/n_c = 4/3$, in which the f and c electrons are diluted, and the data reported are obtained from different numbers of disorder realizations within the statistical errors.

temperature is lowered, the correlation length ξ associated with spin correlations grows, but it is limited by the finite size of the system. Figures 3(a)–3(d) illustrate this for the AF structure factor, plotted as a function of the inverse temperature, $\beta = 1/T$, for different lattice sizes L and U_f, fixing $V = 1$. At high temperatures (small β), $S^{\rm ff}(\pi,\pi)$ is independent of lattice size due to the short-range character of the spin correlations. As β increases, ξ grows, ultimately reaching the linear lattice size L, so that the structure factor increases and stabilizes at a finite value. The growth of $S^{\rm ff}(\pi,\pi)$ with L at low temperatures suggests the existence of long-range order, which should be verified through scaling arguments, as discussed below. Figures 3(e) and 3(f) show that the behavior for the diluted cases is similar, irrespective of n_f being larger or smaller than n_c.

There are several additional features of Fig. 3 which are worth noting: Most importantly, by comparing Figs. 3(b) and 3(e), we see that dilution of conduction orbitals enhances the AF structure factor, as it should. Second, the AF structure factor decreases as U_f decreases, due to the magnitude of the local moments getting smaller as a result of increasing charge fluctuations. For instance, $U_f = 2$ requires larger β to reach the ground state than $U_f = 5$. In fact, since the AF exchange in the Heisenberg limit is $J \sim t^2/U_f$, a large β is also required for $U_f \gg W = 8t$ (not shown).

We probe the existence of long-range ordering by performing a finite-size scaling (FSS) analysis of the structure factor. According to spin-wave theory [72], the AF structure factor scales with system size as

$$\frac{1}{N}S^{\rm ff}(\pi,\pi) = \frac{1}{3}m^2 + \frac{a}{L}, \tag{5}$$

with m^2 being the square of the AF order parameter, and $N = N_f$. Figure 4 exhibits this FSS for different values of U_f and V, for the undiluted PAM. It is interesting to notice that despite the NN hybridization, our results are similar to those of the on-site case [20,31]. Our data suggest that the AF-singlet QCP is located at $V_c \simeq 1.3$, 1.2, 1.0, 0.9, and 0.8 (each estimate carries a rough error bar of 0.05), for $U_f = 6$, 5, 4, 3, and 2, respectively. Also, similarly to the on-site case, V_c for the undiluted PAM is not too sensitive to the value of

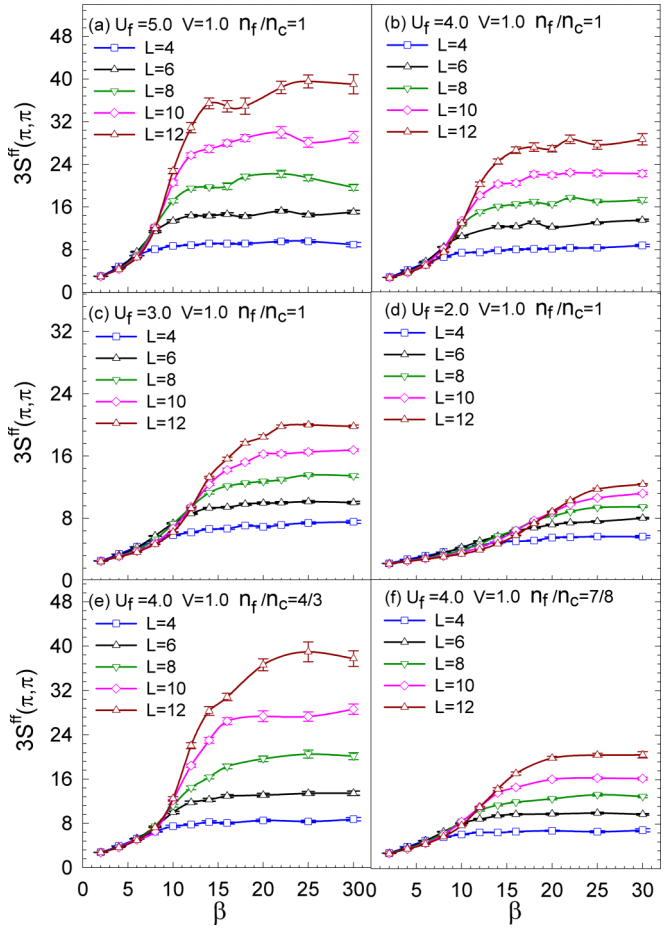

FIG. 3. (a)–(d) Evolution of the AF structure factor, in the absence of any dilution, with increasing β for $V = 1$ and different lattice sizes. Results for $U_f = 5, 4, 3, 2$. As U_f decreases from $U_f = 5$, larger β values are required for $S(\pi,\pi)$ to converge to the ground-state limit. The growth of $S(\pi,\pi)$ with lattice size suggests that there may be long-range AF order for this value of fd hybridization for all the U_f shown. (e),(f) Analogous results for $n_f \neq n_c$ at $U_f = 4$.

U_f; it only changes by approximately 50% over a range where U_f is increased by a factor of three.

We now turn our attention to the FSS analysis for the diluted system, starting with the case $n_f < n_c$ (opposite to the exhaustion limit); see, e.g., Fig. 1(b). Here we take $q = n_f/n_c = 7/8$, with the number of c orbitals being L^2. Following the preceding analyses, Figs. 5(a)–5(e) display the data for different values of U_f and V. A comparison with Fig. 4 reveals that the critical points $V_c(U_f)$ are very close to those for the undiluted case. As expected, the absence of some local moments *reduces* the V required to destroy AF order, but the effect is around 10%, i.e., of the order of $1 - n_f/n_c$. This may be attributed to the longer-range character of the effective RKKY interaction between the local moments.

On the other hand, the exhaustion scenario $n_f/n_c > 1$ is dramatically different. For instance, Fig. 6 presents the scaling analysis for $n_f/n_c = 4/3$, corresponding to one-quarter of the conduction orbitals removed. It is quite evident that when the number of localized electrons is larger than the conduction ones, the AF-singlet quantum critical point is

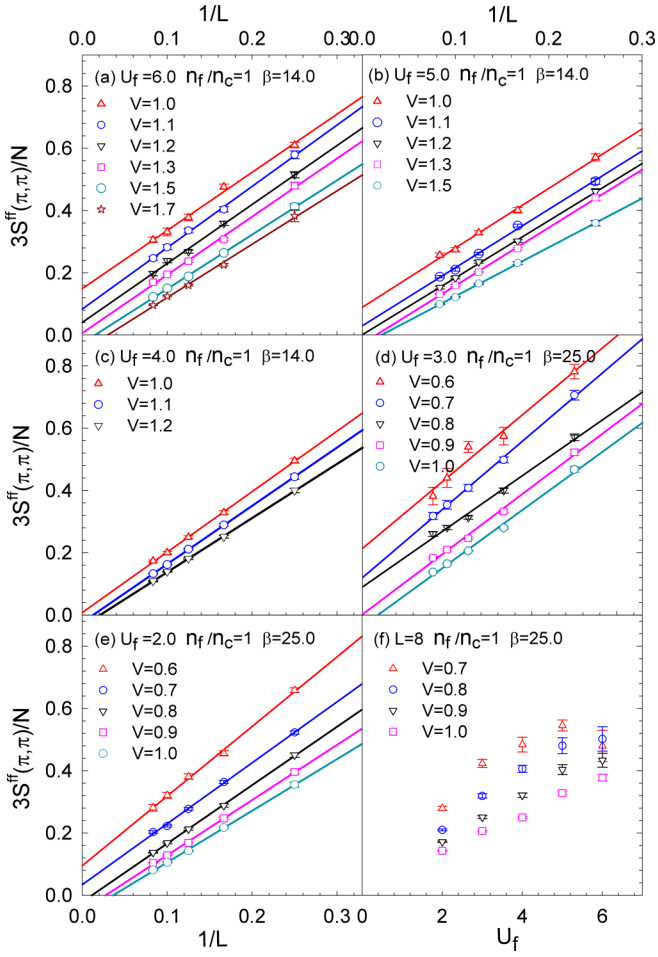

FIG. 4. (a)–(e) Finite-size scaling of the structure factor $S(\pi,\pi)$ when $q \equiv n_f/n_c = 1$. The data suggest values for the AF-singlet QCP $V_c \simeq 1.3, 1.2, 1.0, 0.9$, and 0.8 (each estimate carries a rough error bar of 0.05), for $U_f = 6, 5, 4, 3$, and 2, respectively. These are consistent with the literature. (f) $S^{\rm ff}(\pi,\pi)$ vs U_f for a fixed lattice size $L = 8$ and several values of V.

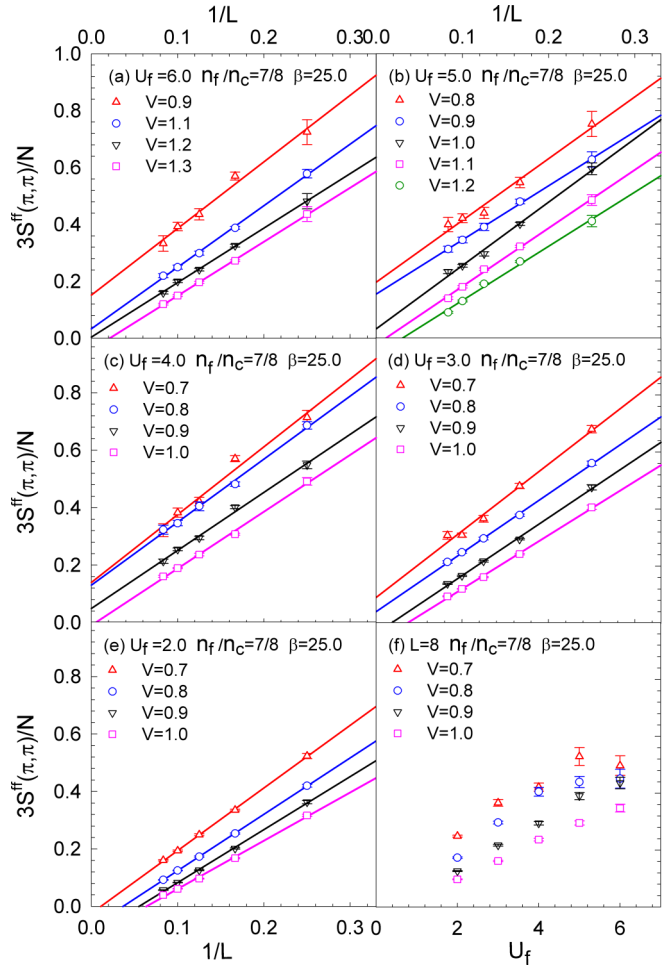

FIG. 5. (a)–(e) Finite-size scaling of the structure factor $S(\pi,\pi)$ when local moments are removed from the lattice, as in Fig. 1(b). The dilution fraction is $q \equiv n_f/n_c = 7/8$. The critical values for the AF-singlet QCP are somewhat reduced by the lower density of magnetic moments. We estimate $V_c \simeq 1.2, 1.1, 0.9, 0.8, 0.6$ (each estimate carries a rough error bar of 0.05), for $U_f = 6, 5, 4, 3, 2$, respectively. (f) $S^{\rm ff}(\pi,\pi)$ vs U_f for a fixed lattice size $L = 8$ and several values of V.

shifted to much larger values of V: long-range AF ordering is stabilized for $V \lesssim 2$ when $U_f = 4$, and for $V \lesssim 3$ when $U_f = 5$. This should be contrasted with the small changes [relative to the undiluted $V_c(U_f)$] that occur when $n_f/n_c < 1$ or which accompany altering U_f at $n_c/n_f = 1$.

Figures 4(f), 5(f), and 6(f) share the feature that the AF structure factor $S^{\rm ff}(\pi,\pi)$ grows monotonically with U_f. We expect that at fixed inverse temperature β, these curves will eventually turn over and decrease, owing to the $1/U_f$ behavior of the exchange constant at strong coupling. In the single-band Hubbard model, maximal AF correlations occur at $U_f \sim 8$ for $\beta \sim 12$ [68]. In summary, from these preceding results, we observe that the critical hybridization for an AF-singlet transition grows dramatically when the conduction-electron count is smaller than the localized ones, while $V_c(U_f)$ is only weakly changed in the opposite situation. All results for the QCP are summarized in the phase diagram of Fig. 7.

We have also investigated the singlet formation by calculating the local singlet correlator, given by Eq. (4). Figure 8 shows C_{fc} as a function of V, that is, as the AF-singlet transition is traversed, for different values of U_f. Figures 8(a)–8(c) display results for several values of U_f, and for the filling ratios $n_f/n_c = 1$, 7/8, and 4/3, respectively. For these cases, C_{fc} increases in magnitude, from small values to $|C_{fc}| \sim 0.4$, as V changes from $V \sim 0.5$ to $V \sim 1.0$. The curves for the three filling ratios also all exhibit a crossing pattern: At weak hybridization V, C_{fc} is largest in magnitude at weak coupling $U_f = 2$. However, as V increases, C_{fc} becomes largest in magnitude at $U_f = 6$; we interpret this as occurring because large U_f yields the most well-formed moments on the f sites.

We have seen that V_c for the destruction of AF order increases dramatically for the exhaustion value, $n_f/n_c = 4/3$, when n_f exceeds n_c. It is intriguing that in Fig. 8, there is not as great a reflection of this in the values of V at which singlet correlators develop. That is, $|C_{fc}|$ grows from small values to $|C_{fc}| \sim 0.4$ in the same range $0.5 \lesssim V \lesssim 1.0$ for

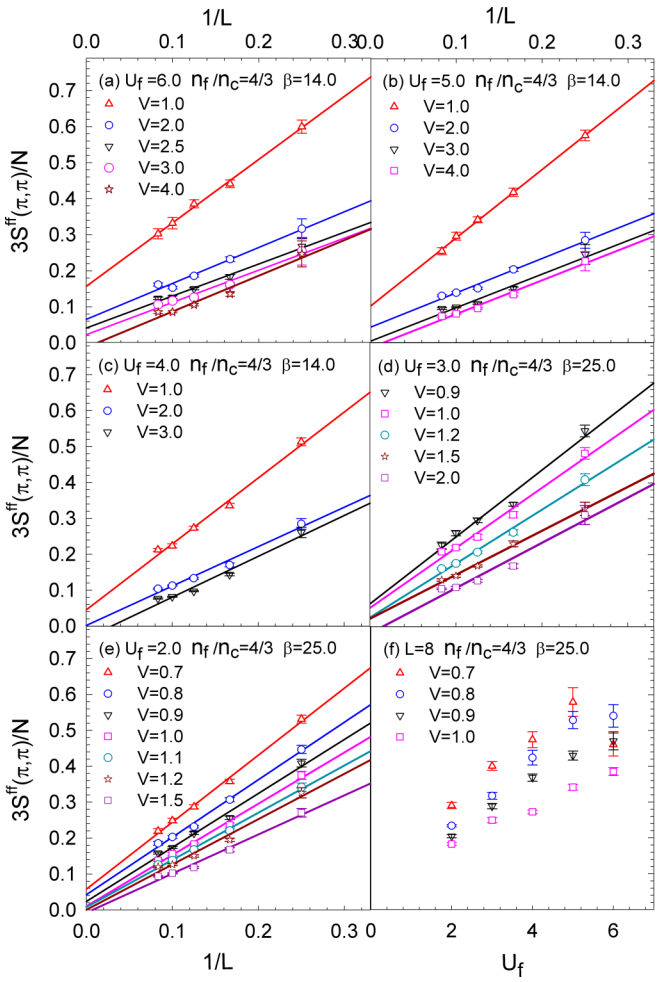

FIG. 6. (a)–(e) Finite-size scaling of the structure factor $S(\pi,\pi)$ when conduction orbitals are removed, as in Fig. 1(c). The ratio of f to c orbitals is $q \equiv n_f/n_c = 4/3$. Especially for larger $U_f = 6, 5, 4$, "exhaustion" has enhanced V_c substantially: $V_c \simeq 3.5, 3.0, 2.0, 1.5, 1.2$ (each estimate carries a rough error bar of 0.05), for $U_f = 6.0, 5.0, 4.0, 3.0, 2.0$. (f) $S^{\rm ff}(\pi,\pi)$ vs U_f for a fixed lattice size $L = 8$ and several values of V.

$n_f/n_c = 4/3$ as for $n_f/n_c = 7/8$ and 1. It appears, therefore, that the interval from $V \sim 1$ to $V_c \sim 3$ (for $U_f = 5, 6$) is characterized by relatively large values of the singlet correlator, even though AF order remains. Whether it corresponds to a partially screened region with coexistence between singlet and AF is a challenge to resolve conclusively with the DQMC methodology used here. While not evident in the onset of C_{fc}, the enhancement of V_c by exhaustion appears to be reflected in the nonmonotonic evolution of C_{fc}, which is unique to the $n_f/n_c = 4/3$ case; see, e.g., Fig. 8(c). The similarity of evolution of the onset for the three filling ratios is emphasized by replotting the data of Figs. 8(a)–8(c) for all three ratios (at a single value $U_f = 4$) in Fig. 8(d).

The data shown in Fig. 8 result from averaging C_{fc} over all f orbitals. However, as discussed in relation to Eq. (2), diluting conduction electrons leads to nonequivalent f orbitals, depending on the number of active connected c sites. Data for C_{fc} can therefore be decomposed according to whether this

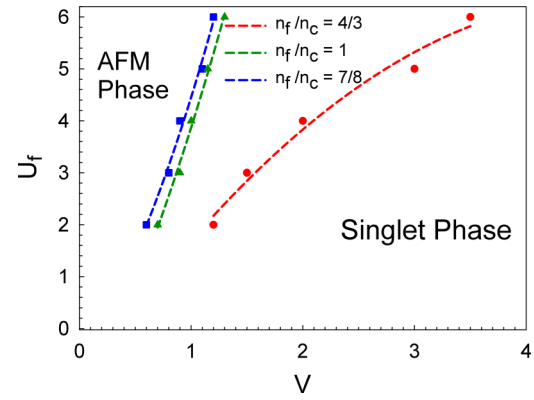

FIG. 7. The ground-state phase diagram. Green triangles mark the AF-singlet transition boundary at $n_f/n_c = 1$, the conventional (i.e., undiluted) periodic Anderson model. The blue squares indicate the boundary for $n_f/n_c = 7/8$, with dilution of *local* electrons. Very little change is noted. Red circles indicate the boundary for $n_f/n_c = 4/3$, dilution of *conduction* electrons, when exhaustion is present. In this case, the stability of AF is dramatically increased.

number is 1, 2, 3, or 4 (the largest value for a square lattice with only near-neighbor f-c hopping). These are, respectively, denoted by $1n$, $2n$, $3n$, $4n$ in Fig. 9. We show this only for the case of exhaustion, $n_f/n_c = 4/3$. As it might have been intuitively expected, C_{fc} is largest in magnitude for $4n$ and smallest for $1n$. It appears that C_{fc} also begins to grow in magnitude at smaller V for $4n$ than for $1n$.

Figure 10 shows the behavior of the double occupancy, $D_\alpha = \langle n^\alpha_{i\uparrow} n^\alpha_{i\downarrow} \rangle$, $\alpha = c$ or f, with V for $U_f = 3$ and $U_f = 5$;

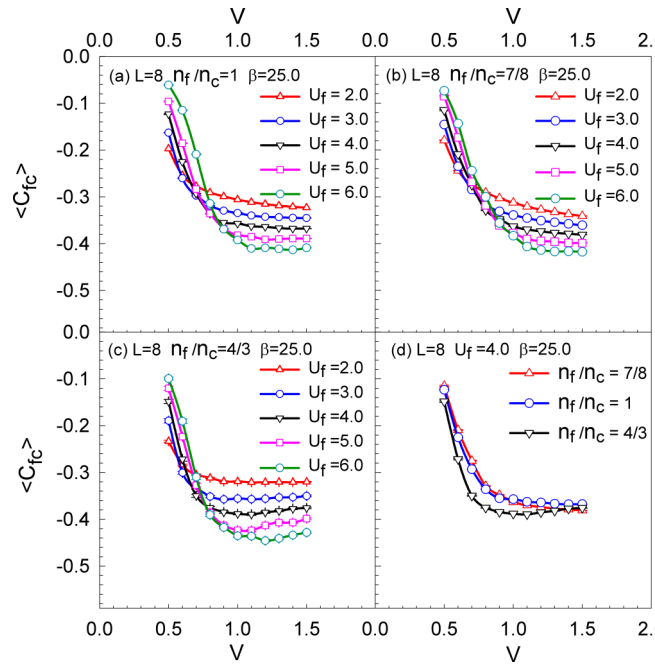

FIG. 8. (a)–(c) The behavior of the singlet correlator as a function of V for different U_f and the three ratios $n_f/n_c = 1, 7/8, 4/3$. The lattice size $L = 8$ and inverse temperature $\beta = 25$. There is a general tendency for singlet formation to occur at $V \sim 0.5$–1.0 for all three filling ratios, as emphasized in (d).

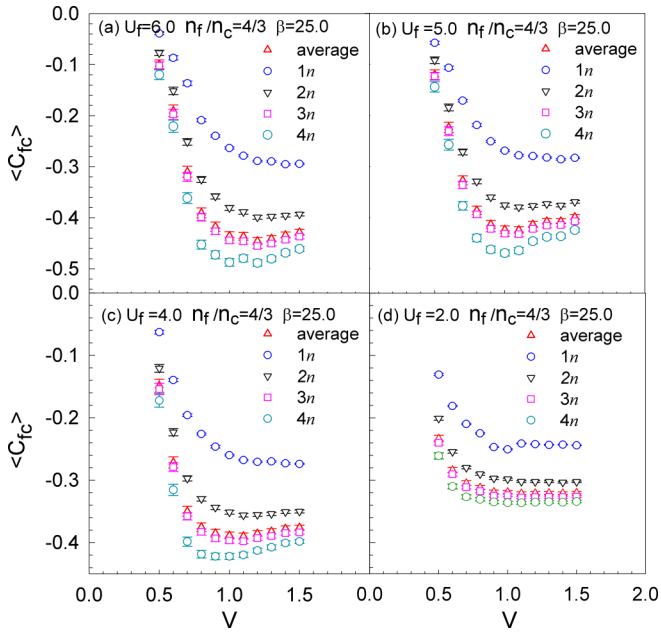

FIG. 9. The singlet correlators for different numbers of conduction electron neighbors are shown as a function of V for the filling ratio $n_f/n_c = 4/3$ which realizes exhaustion. $1n$, $2n$, $3n$, and $4n$ correspond to f orbitals connected to 1, 2, 3, and 4 conduction orbitals by V.

Figs. 10(a) and 10(c) show D_f, while Figs. 10(b) and 10(d) show D_c. The on-site repulsion U_f makes D_f small, especially at small V where quantum fluctuations are suppressed. By contrast, D_c changes very little over the range of V examined, taking on values close to the uncorrelated limit, $D_c \sim \langle n^d_{\mathbf{i}\uparrow}\rangle\langle n^d_{\mathbf{i}\downarrow}\rangle \sim 1/4$.

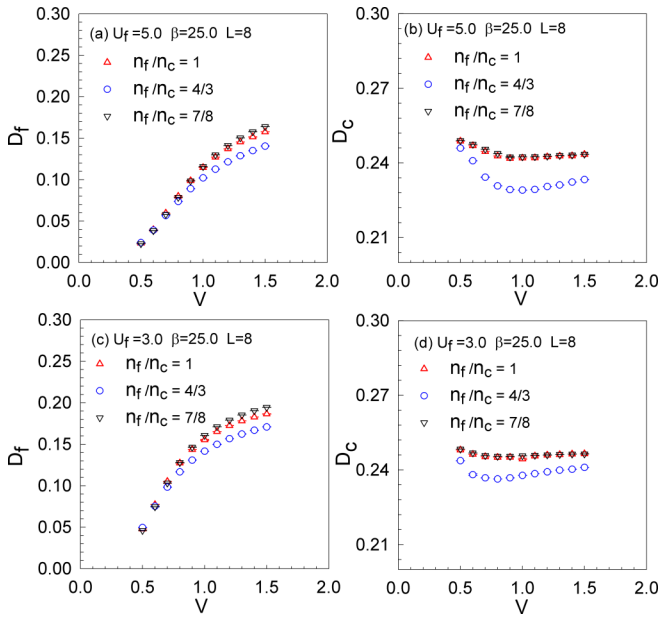

FIG. 10. Double occupancy $D_f(D_c)$ on the $f(c)$ sites vs hybridization V. Larger V results in an increase in D_f. Conduction-electron dilution ($n_f/n_c = 4/3$) is correlated with smaller D_f: there are fewer conduction electrons to hop onto the f orbitals. D_c is roughly at the noninteracting value $1/4$ for all situations.

IV. CONCLUSIONS

One of the quantitative conclusions of past QMC studies of the PAM (in its different variants) is that the position of the QCPs, which signal the AF-singlet transition in the ground state, is rather weakly dependent on the parameters of the model, especially on the value of the on-site repulsion U_f. This was noted in Refs. [20,31], where the phase boundaries were found to be rather vertical in the $U_f - V$ plane, in contrast with mean-field-theory predictions of much larger dV_c/dU_f. Neither V_c was found to vary much in going from two dimensions (2D) to 3D [58], or with changes in the momentum dependence of the f-c hybridization [58,59]. In the former case, the noninteracting density of states is divergent at half filling for 2D and finite for 3D. In the latter case, the on-site and intersite forms for $V_{\mathbf{k}}$ give rise to very different band structures: insulating for V independent of $\mathbf{k}$, and metallic for nearest-neighbor hybridization. Despite these seemingly important differences, V_c was found to be not only rather immune to changes in U_f, but also insensitive to the underlying band structure.

By contrast, one of our key results here, then, is that V_c can vary dramatically with the ratio n_c/n_f. This effect is summarized in the phase diagram in Fig. 6. The physics of exhaustion is starkly evident. While dilution of *local* electrons barely shifts the phase boundary (singlet formation occurs slightly earlier), dilution of *conduction* electrons delays singlet formation to values of V as much as a factor of three greater than in the balanced case, the conventional PAM. This result has the potential to lend qualitative insight into heavy fermion materials since their doping can proceed both by the elimination of moments, e.g., $Ce_{1-x}La_xCoIn_5$, and also by changes to the conduction electrons, e.g., $CeCo_{1-x}Cd_xIn_5$. Theoretical descriptions of the latter situation have focused on the impurity-induced changes to the hybridization V rather than changes to n_c.

A second key, and rather unexpected, conclusion is that in the interval $1 \lesssim V \lesssim 3$ in which exhaustion induces AF order (for $U_f = 5$), the singlet correlator is large. In the undiluted case, the same V_c pinpoints where the AF structure factor becomes small and the singlet correlator becomes large. In the presence of exhaustion, however, these two events no longer share a common V_c and there is an extended region where both $|C_{fc}|$ is large *and* AF order is still present.

The large increase in V_c found for $n_f/n_c > 1$ reflects a significant increase in the stability of the AF phase, the mechanism of which can be attributed to the increased difficulty of forming singlets when the number of conduction electrons available for screening is reduced. Although we have not evaluated T_K and T_{coh} here (it is possible to do so with QMC in the impurity limit using, e.g., the Hirsch-Fye method [73], but much harder for the lattice), it is reasonable to suppose that these temperatures will be reduced to reflect the decreased tendency towards forming singlets. We have also emphasized that the ground-state structure factor $S^{ff}(\pi,\pi)$ is larger for $n_f/n_c = 4/3$ than for $n_f/n_c = 1$, consistent with the general trend towards stronger AF with (a moderate degree of) exhaustion.

The focus of this paper has been on the competition of AF order and singlet formation (for both the cases $n_f/n_c > 1$

and $n_f/n_c < 1$). The physics of exhaustion appears as a large increase in AF stability. It is worth noting that the PAM has also been extensively studied as a model of ferromagnetism (FM) [74,75]. The Nagaoka theorem notwithstanding, FM appears to be very difficult to be achieved in single-band systems such as those described by the Hubbard Hamiltonian. Exploration of $\mathbf{q} = 0$ order would be an interesting avenue to pursue, e.g., in a more extreme limit $n_f/n_c \gg 1$ than that considered here.

ACKNOWLEDGMENTS

L.Z. and T.M. were supported by NSFC (Grant No. 11774033) and Beijing Natural Science Foundation (Grant No. 1192011). The numerical simulations in this work were performed on the HSCC of Beijing Normal University and Tianhe in Beijing Computational Science Research Center. N.C.C. and R.R.dS. acknowledge support by the Brazilian agencies CAPES, CNPq, and FAPERJ. The work of R.T.S. was supported by Grant No. DOE-DE-SC0014671.

[1] P. W. Anderson, Phys. Rev. **124**, 41 (1961).
[2] G. R. Stewart, Rev. Mod. Phys. **56**, 755 (1984).
[3] P. Nozieres, Ann. De Phys. **10**, 19 (1985).
[4] P. A. Lee, T. M. Rice, J. W. Serene, L. J. Sham, and J. W. Wilkins, Comments Condens. Matter Phys. **12**, 99 (1986).
[5] N. Andrei, K. Furuya, and J. H. Lowenstein, Rev. Mod. Phys. **55**, 331 (1983).
[6] P. Schlottmann, Phys. Rev. B **36**, 5177 (1987).
[7] M. A. Ruderman and C. Kittel, Phys. Rev. **96**, 99 (1954).
[8] T. Kasuya, Prog. Theor. Phys. **16**, 45 (1956).
[9] K. Yosida, Phys. Rev. **106**, 893 (1957).
[10] J. C. Xavier, E. Miranda, and E. Dagotto, Phys. Rev. B **70**, 172415 (2004).
[11] R. Peters and N. Kawakami, Phys. Rev. B **92**, 075103 (2015).
[12] N. C. Costa, J. P. Lima, and R. R. dos Santos, J. Magn. Magn. Mater. **423**, 74 (2017).
[13] P. Igoshev, M. Timirgazin, A. Arzhnikov, T. Antipin, and V. Irkhin, J. Magn. Magn. Mater. **440**, 66 (2017).
[14] Y. Zhong, W.-W. Yang, J. Zhao, and H.-G. Luo, arXiv:1903.05295.
[15] N. S. Vidhyadhiraja and D. E. Logan, Eur. Phys. J. B **39**, 313 (2004).
[16] A. C. Hewson, *The Kondo Problem to Heavy Fermions*, Cambridge Studies in Magnetism (Cambridge University Press, Cambridge, England, 2003).
[17] H. Tsunetsugu, M. Sigrist, and K. Ueda, Rev. Mod. Phys. **69**, 809 (1997).
[18] T. M. Rice and K. Ueda, Phys. Rev. Lett. **55**, 995 (1985).
[19] T. M. Rice and K. Ueda, Phys. Rev. B **34**, 6420 (1986).
[20] M. Vekić, J. W. Cannon, D. J. Scalapino, R. T. Scalettar, and R. L. Sugar, Phys. Rev. Lett. **74**, 2367 (1995).
[21] M. Jarrell, Phys. Rev. B **51**, 7429 (1995).
[22] M. J. Rozenberg, Phys. Rev. B **52**, 7369 (1995).
[23] A. Georges, G. Kotliar, W. Krauth, and M. J. Rozenberg, Rev. Mod. Phys. **68**, 13 (1996).
[24] A. N. Tahvildar-Zadeh, M. Jarrell, and J. K. Freericks, Phys. Rev. B **55**, R3332 (1997).
[25] N. S. Vidhyadhiraja, A. N. Tahvildar-Zadeh, M. Jarrell, and H. R. Krishnamurthy, Europhys. Lett. **49**, 459 (2000).
[26] T. Pruschke, R. Bulla, and M. Jarrell, Phys. Rev. B **61**, 12799 (2000).
[27] S. Capponi and F. F. Assaad, Phys. Rev. B **63**, 155114 (2001).
[28] A. Benlagra, T. Pruschke, and M. Vojta, Phys. Rev. B **84**, 195141 (2011).
[29] W. Wu and A.-M.-S. Tremblay, Phys. Rev. X **5**, 011019 (2015).
[30] M. W. Aulbach, F. F. Assaad, and M. Potthoff, Phys. Rev. B **92**, 235131 (2015).
[31] W. Hu, R. T. Scalettar, E. W. Huang, and B. Moritz, Phys. Rev. B **95**, 235122 (2017).
[32] T. Schäfer, A. A. Katanin, M. Kitatani, A. Toschi, and K. Held, arXiv:1812.03821.
[33] D. Meyer and W. Nolting, Phys. Rev. B **61**, 13465 (2000).
[34] Y. Ono, K. Miura, T. Matsuura, and Y. Kuroda, Physica C (Amsterdam) **185–189**, 1669 (1991).
[35] S. Nakatsuji, D. Pines, and Z. Fisk, Phys. Rev. Lett. **92**, 016401 (2004).
[36] N. J. Curro, B.-L. Young, J. Schmalian, and D. Pines, Phys. Rev. B **70**, 235117 (2004).
[37] Y.-F. Yang and D. Pines, Phys. Rev. Lett. **100**, 096404 (2008).
[38] Y.-F. Yang, Z. Fisk, H.-O. Lee, J. Thompson, and D. Pines, Nature (London) **454**, 611 (2008).
[39] K. R. Shirer, A. C. Shockley, A. P. Dioguardi, J. Crocker, C. H. Lin, N. Roberts Warren, D. M. Nisson, P. Klavins, J. C. Cooley, Y.-F. Yang, and N. J. Curro, Proc. Natl. Acad. Sci. USA **109**, E3067 (2012).
[40] S. Wirth and F. Steglich, Nat. Rev. Mater. **1**, 16051 (2016).
[41] Y.-F. Yang, D. Pines, and G. Lonzarich, Proc. Natl. Acad. Sci. USA **114**, 6250 (2017).
[42] M. Jiang, N. J. Curro, and R. T. Scalettar, Phys. Rev. B **90**, 241109(R) (2014).
[43] M. Jiang and Y.-F. Yang, Phys. Rev. B **95**, 235160 (2017).
[44] N. C. Costa, T. Mendes-Santos, T. Paiva, N. J. Curro, R. R. dos Santos, and R. T. Scalettar, Phys. Rev. B **99**, 195116 (2019).
[45] P. Nozieres, Eur. Phys. J. B **6**, 447 (1998).
[46] R. K. Kaul and M. Vojta, Phys. Rev. B **75**, 132407 (2007).
[47] H. Watanabe and M. Ogata, Phys. Rev. B **81**, 113111 (2010).
[48] S. Burdin and C. Lacroix, arXiv:1810.05383.
[49] R. Blankenbecler, D. J. Scalapino, and R. L. Sugar, Phys. Rev. D **24**, 2278 (1981).
[50] J. E. Hirsch, Phys. Rev. B **31**, 4403 (1985).
[51] S. R. White, D. J. Scalapino, R. L. Sugar, E. Y. Loh, J. E. Gubernatis, and R. T. Scalettar, Phys. Rev. B **40**, 506 (1989).
[52] F. Assaad, in *Quantum Simulations of Complex Many-Body Systems: From Theory to Algorithms*, edited by J. Grotendorst, D. Marx, and A. Muramatsu (NIC Series, Jülich, Germany, 2002), Vol. 10, pp. 99–156.
[53] R. R. dos Santos, Braz. J. Phys. **33**, 36 (2003).
[54] J. Gubernatis, N. Kawashima, and P. Werner, *Quantum Monte Carlo Methods: Algorithms for Lattice Models* (Cambridge University Press, Cambridge, England, 2016).
[55] E. Y. Loh, J. E. Gubernatis, R. T. Scalettar, S. R. White, D. J. Scalapino, and R. L. Sugar, Phys. Rev. B **41**, 9301 (1990).
[56] M. Troyer and U.-J. Wiese, Phys. Rev. Lett. **94**, 170201 (2005).
[57] L.-y. Wei and Y.-f. Yang, Sci. Rep. **7**, 46089 (2017).

[58] C. Huscroft, A. K. McMahan, and R. T. Scalettar, Phys. Rev. Lett. **82**, 2342 (1999).
[59] K. Held, C. Huscroft, R. T. Scalettar, and A. K. McMahan, Phys. Rev. Lett. **85**, 373 (2000).
[60] I. Titvinidze, A. Schwabe, and M. Potthoff, Phys. Rev. B **90**, 045112 (2014).
[61] I. Titvinidze, A. Schwabe, and M. Potthoff, Eur. Phys. J. B **88**, 9 (2015).
[62] M. W. Aulbach, I. Titvinidze, and M. Potthoff, Phys. Rev. B **91**, 174420 (2015).
[63] A. Benali, Z. J. Bai, N. J. Curro, and R. T. Scalettar, Phys. Rev. B **94**, 085132 (2016).
[64] N. C. Costa, M. V. Araújo, J. P. Lima, T. Paiva, R. R. dos Santos, and R. T. Scalettar, Phys. Rev. B **97**, 085123 (2018).
[65] H. Trotter, Proc. Am. Math. Soc. **10**, 545 (1959).
[66] M. Suzuki, Prog. Theor. Phys. **56**, 1454 (1976).
[67] R. M. Fye, Phys. Rev. B **33**, 6271 (1986).
[68] R. T. Scalettar, R. M. Noack, and R. R. P. Singh, Phys. Rev. B **44**, 10502 (1991).
[69] R. Mondaini, K. Bouadim, T. Paiva, and R. R. dos Santos, Phys. Rev. B **85**, 125127 (2012).
[70] V. I. Iglovikov, E. Khatami, and R. T. Scalettar, Phys. Rev. B **92**, 045110 (2015).
[71] N. D. Mermin and H. Wagner, Phys. Rev. Lett. **17**, 1133 (1966).
[72] D. A. Huse, Phys. Rev. B **37**, 2380 (1988).
[73] J. E. Hirsch and R. M. Fye, Phys. Rev. Lett. **56**, 2521 (1986).
[74] D. Meyer and W. Nolting, Eur. Phys. J. B **18**, 385 (2000).
[75] C. D. Batista, J. Bonča, and J. E. Gubernatis, Phys. Rev. B **68**, 214430 (2003).